Lawrence Berkeley National Laboratory
Recent Work

Title
Inherent Acidity of Perfluorosulfonic Acid Ionomer Dispersions and Implications for Ink Aggregation.

Permalink
https://escholarship.org/uc/item/66h9m907

Journal
The journal of physical chemistry. B, 122(31)

ISSN
1520-6106

Authors
Berlinger, Sarah A
McCloskey, Bryan D
Weber, Adam Z

Publication Date
2018-08-01

DOI
10.1021/acs.jpcb.8b06493

Peer reviewed

Inherent Acidity of Perfluorosulfonic-Acid Ionomer Dispersions and Implications for Ink Aggregation

Sarah A. Berlinger[1,2], Bryan D. McCloskey[1,2], and Adam Z. Weber[2]*

[1]Department of Chemical and Biomolecular Engineering, University of California, Berkeley, California 94720, USA

[2]Energy Technologies Area, Lawrence Berkeley National Laboratory, 1 Cyclotron Road, Berkeley California 94720, USA

Corresponding Author

* Adam Z. Weber. Address: Lawrence Berkeley National Laboratory, 1 Cyclotron Rd. M/S 70R0108B, Berkeley, CA 94720; Phone: 510-486-4000; Email: azweber@lbl.gov

ABSTRACT

Perfluorosulfonic-acid (PFSA) dispersions are used as components in a variety of electrochemical technologies, particularly in fuel-cell catalyst-layer inks. In this study, we characterize dispersions of a common PFSA, Nafion, as well as inks of Nafion and carbon. It is shown that solvent choice affects a dispersion's measured pH, which is found to scale linearly with Nafion loading. Dispersions in water-rich solvents are more acidic than those in propanol-rich solvents: a 90% water versus 30% water dispersion can have up to a 55% measured proton deviation. Furthermore, because electrostatic interactions are a function of pH, these differences affect how particles aggregate in solution. Despite having different water contents, all inks studied demonstrate the same particle size and surface charge trends as a function of pH, thus providing insights into the relative influence of solvent and pH effects on these properties.

INTRODUCTION

Perfluorosulfonic-acid (PFSA) polymers are currently the industry standard for proton-exchange membranes, having application in a wide variety of fields.[1] Notably, they are a critical component in polymer-electrolyte fuel cells, present as the membrane separator and incorporated into the catalyst layer (CL) to both act as a binder and aid in proton and water transport. CLs are made from inks that are colloidal dispersions of solvent(s), PFSA, and catalyst (typically platinum supported on carbon) nanoparticles.

PFSA is a random copolymer with a hydrophobic polytetrafluoroethylene backbone that provides mechanical support, and pendant hydrophilic sulfonic-acid sidechains. PFSA films (like in a CL) are typically prepared from commercial dispersions, which consist of PFSA (usually in its proton form) dispersed in a solvent. PFSA solution morphology is greatly influenced by solvent choice. X-ray and neutron scattering experiments revealed that PFSA exists as rod-like aggregates with radii ~30Å in polar solvents.[2-4] Moreover, different high dielectric constant (ε) solvents (including varying water:alcohol ratios) can cause morphology to change dramatically (rods, swollen clusters, random-coil network, etc.).[5] The water-alcohol-PFSA mixture is particularly relevant because it is the typical solvent of commercial dispersions and CL inks. It has been demonstrated that these different solution-phase morphologies directly impact cast film properties;[6-14] ionomers maintain a memory of these structures.[15]

These solvent effects must also change the interactions driving ionomer-particle aggregation/stability in an ink, because different water:alcohol ratio inks each exhibit different aggregate sizes,[7, 16-22] and once dried, different CL morphology, water uptake, conductivity, etc. have been observed.[8-9, 23-32] Unfortunately, none of these results are directly comparable to each other due to different components studied. While this solvent effect on cast properties has been

established, there is currently a lack of understanding of the interactions between the catalyst, solvent, and PFSA present in the ink.[33] Initial attempts to model ink interactions used theories for general colloidal interactions of particles (DLVO theory) and polymers, with coulombic repulsion and surface-energy terms.[34-35] However, these general polymer interaction forces are most applicable for uncharged polymers existing in good solvents, which is not the case for PFSA in alcohol/water systems. Due to the complicated biphasic nature of PFSA,[1] a complete model describing catalyst particle-PFSA interactions across all relevant concentration ranges does not exist.

Moreover, pH has not been considered explicitly in any previous PFSA dispersion or ink study. In the cast state, it is well documented that PFSA is a solid superacid, with the sidechain pKa reported to be around −6.[36] It is expected that PFSA will also have some acidity in the dispersion state. This inherent acidity is vitally important for understanding the electrostatic interaction in ink systems, because electrostatic repulsion is a function of surface charge, or zeta potential (ζ), and it is well documented that ζ is a strong function of pH (for the case where protons are potential determining ions, which is true for nearly all systems).[37] Therefore, pH is a determining parameter for particle aggregation. In addition, modifying the surface charge of a carbon substrate changes the affinity of PFSA for that surface.[38] However, no previous study has considered how inherent pH will alter surface charge in these systems or if it exists. This paper attempts to remedy this gap by decoupling solvent and pH effects, and examining how each alters the aggregation (electrostatic) behavior of a fuel-cell CL ink.

METHODS

Materials

Nafion (a prototypical PFSA[1]) was used throughout this study to investigate PFSA behavior. Commercial Nafion dispersions (D2021) were obtained from Ion Power, Inc, and diluted to weight percentages varying from 0.05 to 4%. The structure of Nafion is shown in Figure S1. For each weight percent, multiple samples were prepared in different water to n-propanol (nPA) ratios, ranging from 90 to 30% water (balance consisting of nPA). Samples containing less than 30% water were not studied due to pH probe drift caused by dehydration of the glass membrane. nPA (Sigma-Aldrich) was >99.9% purity, and 18 MΩ de-ionized water (MilliPore) was used. pH measurements were taken with an Orion Star A211 pH meter and a ROSS Ultra Triode pH/ATC probe (Thermo Fisher Scientific). The probe was calibrated before each use with appropriate known standards. Samples were stirred at 400 RPM for the course of the pH measurement; most samples equilibrated in less than thirty seconds. All measurements were repeated at least three times; error represents standard deviation of each sample.

pH Measurement

From a physical viewpoint, a pH measurement is a potential difference measurement, which is then converted to pH via the Nernst equation. This can create deviations from ideality, as junction potentials may influence the potential reading of the probe if the sample's solvent does not match that in the reference electrode. However, junction potentials are usually small (on the order of millivolts in water-alcohol systems).[39] Therefore, they can frequently be ignored, particularly in comparing between samples with the same solvent composition. From a theoretical viewpoint, pH is the negative logarithm of proton activity. In a dilute aqueous system with no added salt, the activity coefficient becomes one; only then is pH directly proportional to

5

proton concentration. Activity may be influenced by myriad factors, including solvent Ɛ, degree of solvation/dissociation, etc. Consequently, the meaning of pH becomes a bit confusing as one moves away from aqueous systems; different solvents cannot be readily compared with each other due to different activities associated with those unique environments. Therefore, the pH measurement is a function of both proton concentration and solvent environment.

To alleviate this issue, an acid baseline was studied. Both perchloric (Sigma-Aldrich) and hydrochloric acids (MilliPore Sigma) were used to investigate different anions and confirm the relative insensitivity of the pH measurement with respect to the anion composition if a strong acid is used. The pH of each acid at different concentrations spanning from 0.001 to 0.1M was measured in solvents with water percentages ranging from 100 to 30%. There was little difference between these two acids. Furthermore, within the concentration range measured, there was no dependence of pH offset on concentration (i.e. the expected pH agreed with the measured pH for both 0.1M and 0.001M acid). Each point in the acid baseline (Figure S2) is an average of each concentration for both acids at that given solvent environment. The acid baseline allows one to decouple solvent environment and concentration effects, taking into account the expected pH deviation attributed to a proton existing in a different solvent environment. Total proton concentration is readily calculated given the equivalent weight and dispersion volume; this value was then corrected for solvent environment effects using the acid baseline. This correction is discussed in more detail in the Supporting Information (SI).

Inks

Simplified inks with 0.1 wt% carbon were prepared at ionomer to carbon (I:C) weight ratios from 0 to 1.5, in the same solvent ratios as above, using Vulcan XC72R (Fuel Cell Store). While it is expected that the addition of platinum will alter the results reported here, carbon and

ionomer inks were chosen to initially understand the binary ionomer/carbon interaction. Primary carbon particles were 50nm in diameter. All samples (dispersions and inks) were mechanically stirred for twenty minutes and then sonicated in a bath sonicator (Branson) for one hour. During the sonication, bath temperature remained constant via a water recirculator/chiller. Immediately after sonication, samples were measured via dynamic and electrophoretic light scattering (DLS, ELS, respectively, Nanoplus3, Micromeritics) to determine aggregation diameter and ζ. Aggregate diameter was determined via the Stokes-Einstein equation (DLS measures a diffusion coefficient, which can then be related to a hydrodynamic radius via Stokes-Einstein), and ζ was modeled with the Smoluchowski equation (aggregates have sufficiently large values of $\varkappa a$ such that the Smoluchowski equation is valid, in which $\varkappa$ is the inverse Debye length and a is the particle radius).[37] Other models do exist for soft particles (i.e. polymer layer covering a hard sphere) but they provide marginal corrections at the length scale of interest in this system.[40-42]

To decouple pH/solvent effects, dispersions in different solvent ratios were prepared, and acid ($HClO_4$) or base (NaOH) was added such that all dispersions had the same pH. Tested pHs were 0, 1, 2.5, and 9. pH 0 is below the isoelectric point of carbon (shown in Figure S3 to be around 1), and pH 2.5 is similar to that expected of a typical ink. Inks were then prepared from these pH-normalized dispersions. I:C ratios of 0 were not studied fully at all of these pHs because they were unstable and immediately aggregated (Figure S3). Meanwhile, all inks with appreciable ionomer levels show stability.

RESULTS AND DISCUSSION

Dispersion pH

First, it is necessary to understand the ionomer/solvent interaction in terms of pH: to determine how varying water:nPA ratios change the pH of a dispersion for a given PFSA concentration, as well as how pH is affected by PFSA concentration for a given solvent ratio. The measured pH of PFSA dispersions diluted to different concentrations in solvents containing 90, 70, 50, and 30% water (balance nPA) is plotted in Figure 1. Each solvent ratio shows a linear dependence of pH on Nafion concentration, where the Nafion loadings are chosen to represent those occurring in different CL fabrication processes.[33] Furthermore, water-rich dispersions exhibit more acidic behavior, while nPA-rich dispersions are less acidic. The difference between pH for each water ratio at a given Nafion concentration decreases as the amount of Nafion in the dispersion increases (i.e. at 0.05 wt%, the difference between the 90 and 30% water systems is 0.68 pH units, while at 4% the difference is only 0.25).
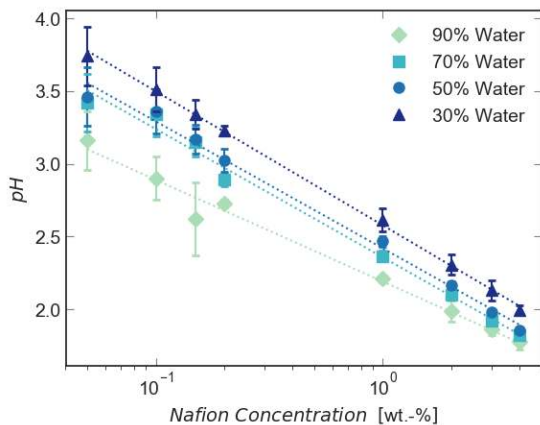

Figure 1. Measured pH of Nafion as a function of Nafion and water concentrations.

This difference is significant, and is better seen in Figure 2, where percent protons measured (PM) is plotted versus water concentration for given Nafion concentrations. PM is calculated by dividing the concentration of measured protons using a pH meter by the corrected total proton concentration expected from Nafion. For dilute Nafion concentrations (0.2 wt% in Figure 2) in

90% water, roughly all of the protons behave as would be expected from an ideal strong electrolyte solution of similar proton concentration (i.e., the measured proton concentration is the same as the total proton concentration). As the fraction of nPA is increased in the solvent, fewer protons (~40% of the theoretical expected amount) are detected at a given Nafion wt%. As Nafion concentration increases, PM decreases, and the difference between varying water contents decreases. Indeed, by 4 wt% Nafion, the PM (40-50%) is not substantially influenced by the solvent water/nPA ratio.
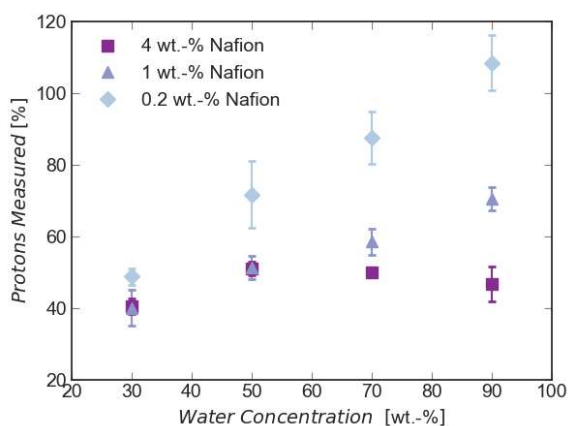

Figure 2. Measured proton divided by corrected theoretical proton concentration as a function of water concentration.

pH deviations seen cannot be due to the fact that propanol is slightly less acidic than water, because strong acids in the same propanol environment experienced little to no pH change (based on the acid baseline measurement). Furthermore, classical polyelectrolyte theories like Manning condensation do not account for deviations, because the charge spacing (taken to be the average backbone spacing between sidechains) is larger than the Bjerrum length for almost all of the

samples.[43] Therefore, if change in measured protons is not due to solvent effects, it is proposed that they are attributed to changes in ionomer conformation.

It has already been discussed that the general structure of PFSA changes in different water:alcohol ratios. Perhaps, pH changes are a result of different sidechain orientations brought about by these different solvent contents. While most sulfonate-proton pairs should be dissociated in aqueous solutions, the protons will still remain within a Bjerrum length (~nm) of the sulfonate anions due to electroneutrality. It is suspected that protons that remain in proximity to sulfonate ions inside the PFSA structure will not participate as dissociated free protons as occur in small molecule strong acids (e.g., HCl). However, in water-rich solvents, which have a higher affinity to the ionic sidechain than organic-rich solvents do, more sidechains will extend into the solvent and a more acidic bulk pH is expected. As propanol content is increased, there is less of a preference for sidechain orientation into solution (an inverted micellar structure has been proposed),[44] and less acidic pHs are measured. Therefore, PM in Figure 2 may be thought of as the number of total protons that are accessible in the bulk solution (versus those that are internal to the aggregate structure).

Moreover, as ionomer concentration is increased, there is less of a difference in accessible protons between varying water contents than at lower concentrations. It is well known that Nafion can form secondary aggregates in solution;[6] at higher Nafion concentrations, a large portion of sidechains already exist inside the aggregate structure and therefore have buried sulfonate-proton pairs. Since there are less accessible protons, a lower percentage of the total protons in the dispersion is measured, even for very high water contents, and the effect of nPA content has a less dramatic effect than it does for very low Nafion concentrations. A schematic of the proposed preceding sidechain reorientation argument is shown in Figure 3. Additional

experimental structural observations would be necessary to definitively confirm this theory, but current experimental techniques lack resolution required to resolve backbone and sidechain orientation. Cryo-transmission electron micrographs of Nafion dispersions are shown in the SI. From the images, in propanol-rich solvents, PFSA forms narrow rod-like aggregates (with sidechains probably internal to the aggregate) and in water-rich solvents the hydrophobic backbone clusters in the middle of the aggregate.
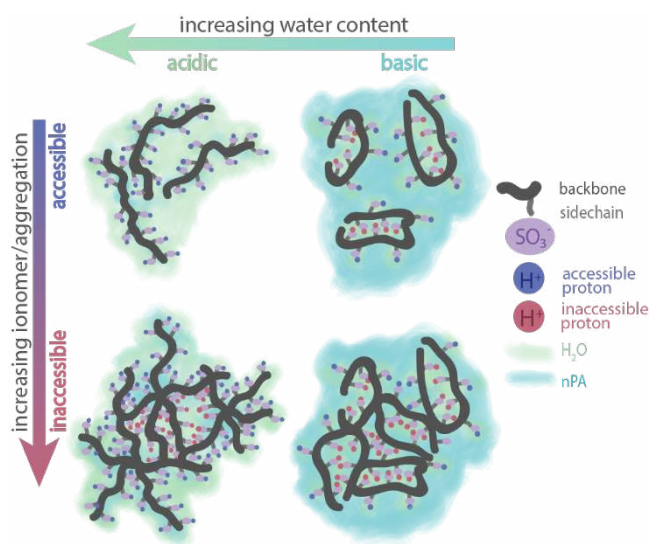

Figure 3. Schematic of 2D slice of potential structure representing individual chains and aggregates of Nafion, showing the sidechain orientation differences (pH differences) as a function of aggregation and solvent content.

Ink Aggregation

The above describes the interrelationship between pH and PFSA loading in dispersions, but there is a need to explore these effects in the tertiary ionomer/solvent/particle ink system. To do this, simplified inks containing Vulcan carbon, Nafion, and varying nPA:water and I:C ratios were fabricated as described in the Methods section.

The effect of Nafion concentration on pH in a carbon-solvent system is shown in Figure 4, where carbon suspensions are essentially titrated using a Nafion dispersion. Here, the measured pH of the total ink is plotted versus the number of measured protons (from Figure 2) associated with the addition of Nafion. The neat carbon particle suspensions all have a pH around 7 to 8, which is expected given the very weakly basic character of typical oxygen defects present on carbon black surfaces.[45] If the Nafion did not interact at all with the carbon, we would expect a linear response similar to Figure 1. However, as Nafion is added, an equivalence point is observed between pH 7 and 4 for all solvent mixtures studied. As the water content increases, the total Nafion required to reach the equivalence point also increases (around an order of magnitude measured proton concentration difference between 30 and 90% water for the same Nafion concentration). This indicates that the magnitude of the electrostatic forces controlling ionomer/carbon interactions are fundamentally different between different solvent types (more charged groups on the ionomer and carbon surface interact in water-rich solvents than propanol-rich). Optimal I:C ratios have previously been thought to be related to how the ionomer covers the carbon. However, ideal I:C ratios seem to vary slightly between groups that report using different solvents and carbon particles.[6, 24, 46-49] Considering this titration behavior, ionomer coverage is most likely related to pH (and different electrostatic magnitude) as a result of changing charge density (ionic strength).
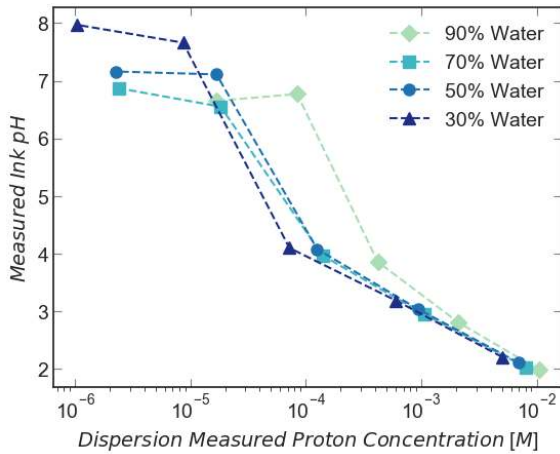
Figure 4. Titration of a 0.1 wt% XC72 Vulcan carbon particle solution by the addition of Nafion (plotted as measured proton concentration) at different water/nPA ratios.

These varying electrostatic interactions will also affect the aggregation behavior of the ink, as shown in Figure 5. High magnitudes of zeta potential (ζ) indicate particles with high electrostatic repulsion, whereas lower values indicate particles are more susceptible to aggregation. With no PFSA, the carbon aggregate diameter increases with increasing water content, probably driven by hydrophobic effects. Upon addition of Nafion, aggregate size continues to increase, while displaying the same water content/size relationship. Because each of these inks are at a different ionomer concentration and solvent ratio, they are each at a different pH (and therefore different charge concentration and magnitude of electrostatic interaction). This is seen in Figure 5b: each ink has a different ζ.
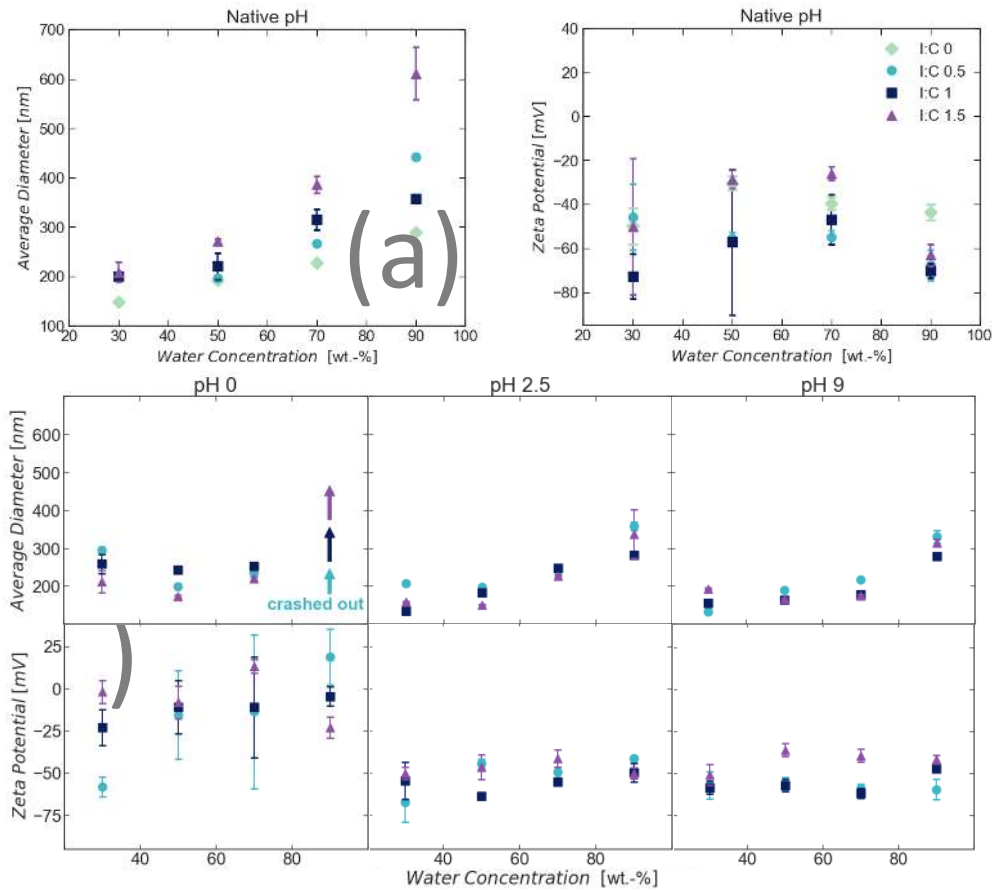
Figure 5. (a) The diameter as measured by dynamic light scattering and (b) zeta potential of the carbon/ionomer aggregates at different water percentages for Ionomer:Carbon (I:C) ratios between 0 and 1.5, without adjusting pH. (c)-(e) The average diameter of inks made by first adjusting the dispersion pH to 0, 2.5, and 9, respectively. (f)-(h) The average zeta potential of the same inks in (c)-(e).

To distinguish between pH and solvent effects on aggregation, dispersion pH (total measured protons) was adjusted to the same value (0, 2.5, or 9) using $HClO_4$ or NaOH, before adding carbon particles. Aggregate size is shown in Figure 5c-e, and ζ in 4f-h for each pH. I:C of zero was not able to be studied fully at any of these pHs because it immediately aggregated and condensed (shown in the SI). This is evidence that Nafion acts as a stabilizing agent for carbon

14

particles (or perhaps buffering agent), in agreement with previously findings that Nafion addition increases stability.[34-35] pH-normalized inks exhibit the same size and ζ trends as a function of I:C. Indeed, there is almost no difference between the I:C ratios, whereas in the native pH state there was over a 300 nm size difference between I:C 0.5 and 1.5 for 90% water.

It is important to note that a number of factors may be influencing the aggregation behavior, including changing dielectric constant and ionic strength. Both of these may be brought about by the addition of either ionomer or acid.[50] However, both of these are closely related to pH in these systems. Dielectric constant and ionic strength may both be changing because of ionic group addition, which is reflected in the dispersion pH. Therefore, even though there may be other indirect effects driving aggregation behavior, they are all ultimately linked to the ionomer dispersion behavior.

Furthermore, similarities between Figures 5d and e could be explained by similarities in ionic strength. Ionic strength is representative of the number of charged ionic species in the system. When the inks are normalized to the same pH, they should also therefore have the same effective ionic strength (they will have different number of accessible protons from the Nafion, and different amounts of added protons from the acid, but they will ultimately have the same acid concentration, and therefore the same ionic strength). Interestingly, when adding base, much more was required than calculated based solely on measured proton concentration. A possible explanation could be sodium ion exchange with the inaccessible protons, thus making the dispersion more acidic than initially measured. Due to this increased amount of base added, the ionic strength of the alkaline and acidic normalized inks was very similar, perhaps explaining similarities in observed aggregate diameters.

For each ink, the ζ is very similar for all I:C ratios, indicating comparable levels of electrostatic interactions. Furthermore, as acid content increases, ζ trends toward zero, even becoming positive for some samples at pH 0, in agreement with typical electrostatically-controlled system behavior. However, it is also evident that hydrophobic effects play a large role in aggregation. As an example, consider the pH 0 graphs (Figure 5c,f) where all of the 90% water samples crash out of solution. The ζ for the 90% water dispersions becomes more negative with increasing I:C (which is also consistent with the idea that sidechains are facing outward and therefore contribute more negative groups once adsorbed to the carbon surface). However, the unstable 1.5 I:C 90% water ink has a larger magnitude ζ than, for example, the stable 1.5 I:C 70% water ink. If the system was purely electrostatically dominated, then the 1.5 I:C 70% water ink should be unstable as well; however, it was stable on the measured timescale (3 hours).

Of additional interest, for the 30% water case, the I:C- ζ trend is reversed, with the lowest I:C ratio exhibiting the most negative ζ. This is consistent with the sidechains having less affinity for nPA than water, and therefore are not exposed on the surface. It is clear that both solvent (in the form of hydrophobic forces) and pH (as a manifestation of PFSA conformation) are coupled and each contribute significantly to the resulting ink-aggregation behavior.

CONCLUSIONS

PFSAs have an inherent pH that is dependent on solvent composition, and may be a result of solvent-induced morphology changes. Indeed, pH could be a simple screening tool for PFSA structural parameters. These different dispersions have varying numbers of accessible protons, which alter the ionic strength and magnitude of electrostatic interaction. In a fuel-cell ink, this manifests in different aggregation behavior that collapses when inks are reduced to the same pH.

The findings presented herein have potentially far-reaching implications for enhanced control over ink properties and engineering for various electrochemical technologies, enabling one to tune both solvent (viscosity, evaporation rate, hydrophobicity) and pH (electrostatic aggregation) effects independently.

ASSOCIATED CONTENT

Supporting Information.

The following files are available free of charge.

pH measurement corrections, cryo-TEM of PFSA dispersions (PDF)

AUTHOR INFORMATION

The authors declare no competing financial interests.

ACKNOWLEDGEMENTS

REFERENCES

1. Kusoglu, A.; Weber, A. Z. New Insights into Perfluorinated Sulfonic-Acid Ionomers. *Chem. Rev.* **2017**, *117*, 987-1104.

2. Loppinet, B.; Gebel, G. Rodlike Colloidal Structure of Short Pendant Chain Perfluorinated Ionomer Solutions. *Langmuir* **1998**, *14*, 1977-1983.

3. Loppinet, B.; Gebel, G.; Williams, C. E. Small-Angle Scattering Study of Perfluorosulfonated Ionomer Solutions. *J. Phys. Chem. B.* **1997**, *101*, 1884-1892.

4. Gebel, G.; Loppinet, B. Colloidal Structure of Ionomer Solutions in Polar Solvents. *J. Mol. Struct.* **1996**, *383*, 43-49.

5. Welch, C.; Labouriau, A.; Hjelm, R.; Orler, B.; Johnston, C.; Kim, Y. S. Nafion in Dilute Solvent Systems: Dispersion or Solution? *ACS Macro. Lett.* **2012**, *1*, 1403-1407.

6. Holdcroft, S. Fuel Cell Catalyst Layers: A Polymer Science Perspective. *Chem. Mater.* **2014**, *26*, 381-393.

7. Ngo, T. T.; Yu, T. L.; Lin, H.-L. Influence of the Composition of Isopropyl Alcohol/Water Mixture Solvents in Catalyst Ink Solutions on Proton Exchange Membrane Fuel Cell Performance. *J. Power Sources* **2013**, *225*, 293-303.

8. Shin, S. J.; Lee, J. K.; Ha, H. Y.; Hong, S. A.; Chun, H. S.; Oh, I. H. Effect of the Catalytic Ink Preparation Method on the Performance of Polymer Electrolyte Membrane Fuel Cells. *J. Power Sources* **2002**, *106*, 146-152.

9. Uchida, M.; Aoyama, Y.; Eda, N.; Ohta, A. New Preparation Method for Polymer-Electrolyte Fuel Cells. *J. Electrochem. Soc.* **1995**, *142*, 463-468.

10. Kim, Y. S.; Welch, C. F.; Hjelm, R. P.; Mack, N. H.; Labouriau, A.; Orler, E. B. Origin of Toughness in Dispersion-Cast Nafion Membranes. *Macromolecules* **2015**, *48*, 2161-2172.

11. Ma, C.-H.; Yu, T. L.; Lin, H.-L.; Huang, Y.-T.; Chen, Y.-L.; Jeng, U. S.; Lai, Y.-H.; Sun, Y.-S. Morphology and Properties of Nafion Membranes Prepared by Solution Casting. *Polymer* **2009**, *50*, 1764-1777.

12. Johnston, C. M.; Lee, K.-S.; Rockward, T.; Labouriau, A.; Mack, N.; Kim, Y. S. Impact of Solvent on Ionomer Structure and Fuel Cell Durability. *ECS Trans.* **2009**, *25*, 1617-1622.

13. Silva, R. F.; De Francesco, M.; Pozio, A. Solution-Cast Nafion® Ionomer Membranes: Preparation and Characterization. *Electrochim. Acta* **2004**, *49*, 3211-3219.

14. Moore, R. B.; Martin, C. R. Chemical and Morphological Properties of Solution-Cast Perfluorosulfonate Ionomers. *Macromolecules* **1988**, *21*, 1334-1339.

15. Lundberg, R. D.; Phillips, R. R. Influence of Sample History on Ionomer Properties. *J. Polym. Sci., Part C: Polym. Lett* **1984**, *22*, 377-384.

16. Zhang, H.; Pan, J.; He, X.; Pan, M. Zeta Potential of Nafion Molecules in Isopropanol-Water Mixture Solvent. *J. Appl. Polym. Sci.* **2008**, *107*, 3306-3309.

17. Lee, S.-J.; Yu, T. L.; Lin, H.-L.; Liu, W.-H.; Lai, C.-L. Solution Properties of Nafion in Methanol/Water Mixture Solvent. *Polymer* **2004**, *45*, 2853-2862.

18. Ngo, T. T.; Yu, T. L.; Lin, H.-L. Nafion-Based Membrane Electrode Assemblies Prepared from Catalyst Inks Containing Alcohol/Water Solvent Mixtures. *J. Power Sources* **2013**, *238*, 1-10.

19. Li, S.; Terao, K.; Sato, T. Colloidal Dispersion of a Perfluorosulfonated Ionomer in Water–Methanol Mixtures. *Polymers* **2018**, *10*, 72.

20. Yang, F.; Xin, L.; Uzunoglu, A.; Qiu, Y.; Stanciu, L.; Ilavsky, J.; Li, W.; Xie, J. Investigation of the Interaction between Nafion Ionomer and Surface Functionalized

Carbon Black Using Both Ultrasmall Angle X-Ray Scattering and Cryo-Tem. *ACS Appl. Mater. Interfaces* **2017**, *9*, 6530-6538.

21. Takahashi, S.; Shimanuki, J.; Mashio, T.; Ohma, A.; Tohma, H.; Ishihara, A.; Ito, Y.; Nishino, Y.; Miyazawa, A. Observation of Ionomer in Catalyst Ink of Polymer Electrolyte Fuel Cell Using Cryogenic Transmission Electron Microscopy. *Electrochim. Acta* **2017**, *224*, 178-185.

22. Xu, F.; Zhang, H.; Ilavsky, J.; Stanciu, L.; Ho, D.; Justice, M. J.; Petrache, H. I.; Xie, J. Investigation of a Catalyst Ink Dispersion Using Both Ultra-Small-Angle X-Ray Scattering and Cryogenic Tem. *Langmuir* **2010**, *26*, 19199-19208.

23. Kim, T.-H.; Yi, J.-Y.; Jung, C.-Y.; Jeong, E.; Yi, S.-C. Solvent Effect on the Nafion Agglomerate Morphology in the Catalyst Layer of the Proton Exchange Membrane Fuel Cells. *Int. J. Hydrogen Energy* **2017**, *42*, 478-485.

24. Zamel, N. The Catalyst Layer and Its Dimensionality – a Look into Its Ingredients and How to Characterize Their Effects. *J. Power Sources* **2016**, *309*, 141-159.

25. Jung, C.-Y.; Kim, W.-J.; Yi, S.-C. Optimization of Catalyst Ink Composition for the Preparation of a Membrane Electrode Assembly in a Proton Exchange Membrane Fuel Cell Using the Decal Transfer. *Int. J. Hydrogen Energy* **2012**, *37*, 18446-18454.

26. Huang, D. C.; Yu, P. J.; Liu, F. J.; Huang, S. L.; Hsueh, K. L.; Chen, Y. C.; Wu, C. H.; Chang, W. C.; Tsau, F. H. Effect of Dispersion Solvent in Catalyst Ink on Proton Exchange Membrane Fuel Cell Performance. *Int. J. Electrochem. Sci.* **2011**, *6*, 2551-2565.

27. Therdthianwong, A.; Ekdharmasuit, P.; Therdthianwong, S. Fabrication and Performance of Membrane Electrode Assembly Prepared by a Catalyst-Coated Membrane Method: Effect of Solvents Used in a Catalyst Ink Mixture. *Energy Fuels* **2010**, *24*, 1191-1196.

28. Thanasilp, S.; Hunsom, M. Effect of Mea Fabrication Techniques on the Cell Performance of Pt–Pd/C Electrocatalyst for Oxygen Reduction in Pem Fuel Cell. *Fuel* **2010**, *89*, 3847-3852.

29. Sung, K. A.; Jung, H.-Y.; Kim, W.-K.; Cho, K.-Y.; Park, J.-K. Influence of Dispersion Solvent for Catalyst Ink Containing Sulfonated Poly(Ether Ether Ketone) on Cathode Behaviour in a Direct Methanol Fuel Cell. *J. Power Sources* **2007**, *169*, 271-275.

30. Fernández, R.; Ferreira-Aparicio, P.; Daza, L. Pemfc Electrode Preparation: Influence of the Solvent Composition and Evaporation Rate on the Catalytic Layer Microstructure. *J. Power Sources* **2005**, *151*, 18-24.

31. Litster, S.; McLean, G. Pem Fuel Cell Electrodes. *J. Power Sources* **2004**, *130*, 61-76.

32. Kim, J.-H.; Ha, H. Y.; Oh, I.-H.; Hong, S.-A.; Lee, H.-I. Influence of the Solvent in Anode Catalyst Ink on the Performance of a Direct Methanol Fuel Cell. *J. Power Sources* **2004**, *135*, 29-35.

33. Hatzell, K. B.; Dixit, M. B.; Berlinger, S. A.; Weber, A. Z. Understanding Inks for Porous-Electrode Formation. *J. Mater. Chem. A* **2017**, *5*, 20527-20533.

34. Dixit, M. B.; Harkey, B. A.; Shen, F.; Hatzell, K. B. Catalyst Layer Ink Interactions That Affect Coatability. *J. Electrochem. Soc.* **2018**, *165*, F264-F271.

35. Shukla, S.; Bhattacharjee, S.; Weber, A. Z.; Secanell, M. Experimental and Theoretical Analysis of Ink Dispersion Stability for Polymer Electrolyte Fuel Cell Applications. *J. Electrochem. Soc.* **2017**, *164*, F600-F609.

36. Sondheimer, S. J.; Bunce, N. J.; Lemke, M. E.; Fyfe, C. A. Acidity and Catalytic Activity of Nafion-H. *Macromolecules* **1986**, *19*, 339-343.

37. Israelachvili, J. N. *Intermolecular and Surface Forces*; Academic Press, 2011; Vol. 3.

38. Koestner, R.; Roiter, Y.; Kozhinova, I.; Minko, S. Effect of Local Charge Distribution on Graphite Surface on Nafion Polymer Adsorption as Visualized at the Molecular Level. *J. Phys. Chem. C.* **2011**, *115*, 16019-16026.

39. Gelsema, W. J.; de Ligny, C. L.; Remijnse, A. G.; Blijleven, H. A. Ph-Measurements in Alcohol-Water Mixtures, Using Aqueous Standard Buffer Solutions for Calibration. *Recueil des Travaux Chimiques des Pays-Bas* **1966**, *85*, 647-660.

40. Dukhin, S. S.; Zimmermann, R.; Werner, C. Electrokinetic Phenomena at Grafted Polyelectrolyte Layers. *J. Colloid Interface Sci.* **2005**, *286*, 761-773.

41. Hiroyuki, O. Theory of Electrostatics and Electrokinetics of Soft Particles. *Science and Technology of Advanced Materials* **2009**, *10*, 063001.

42. Ohshima, H. Electrophoresis of Soft Particles: Analytic Approximations. *ELECTROPHORESIS* **2006**, *27*, 526-533.

43. Manning, G. S. Limiting Laws and Counterion Condensation in Polyelectrolyte Solutions I. Colligative Properties. *The Journal of Chemical Physics* **1969**, *51*, 924-933.

44. Rubatat, L.; Gebel, G.; Diat, O. Fibrillar Structure of Nafion: Matching Fourier and Real Space Studies of Corresponding Films and Solutions. *Macromolecules* **2004**, *37*, 7772-7783.

45. O'Reilly, J. M.; Mosher, R. A. Functional Groups in Carbon Black by Ftir Spectroscopy. *Carbon* **1983**, *21*, 47-51.

46. Ishikawa, H.; Sugawara, Y.; Inoue, G.; Kawase, M. Effects of Pt and Ionomer Ratios on the Structure of Catalyst Layer: A Theoretical Model for Polymer Electrolyte Fuel Cells. *J. Power Sources* **2018**, *374*, 196-204.

47. Mashio, T.; Ohma, A.; Tokumasu, T. Molecular Dynamics Study of Ionomer Adsorption at a Carbon Surface in Catalyst Ink. *Electrochim. Acta* **2016**, *202*, 14-23.

48. Sasikumar, G.; Ihm, J. W.; Ryu, H. Dependence of Optimum Nafion Content in Catalyst Layer on Platinum Loading. *J. Power Sources* **2004**, *132*, 11-17.

49. Antolini, E.; Giorgi, L.; Pozio, A.; Passalacqua, E. Influence of Nafion Loading in the Catalyst Layer of Gas-Diffusion Electrodes for Pefc. *J. Power Sources* **1999**, *77*, 136-142.

50. Fahrenberger, F.; Hickey, O. A.; Smiatek, J.; Holm, C. Importance of Varying Permittivity on the Conductivity of Polyelectrolyte Solutions. *Phys. Rev. Lett.* **2015**, *115*, 118301.

TOC GRAPHIC